**Proceedings of the 19th World Congress**
**The International Federation of Automatic Control**
**Cape Town, South Africa. August 24-29, 2014**

# Stability of Synchronized Motions of Inverter–Based Microgrids Under Droop Control

**Johannes Schiffer** * **Romeo Ortega** ** **Alessandro Astolfi** ***
**Jörg Raisch** *,**** **Tevfik Sezi** ◇

* *Technische Universität Berlin, Germany (e-mail: schiffer@control.tu-berlin.de)*
** *Laboratoire des Signaux et Systémes, SUPELEC, France (e-mail: ortega@lss.supelec.fr)*
*** *Department of Electrical and Electronic Engineering, Imperial College London, London SW7 2AZ, U.K. & Dipartimento di Ing. Civile e Ing. Informatica, University of Rome, Tor Vergata, 00133 Rome, Italy (e-mail: a.astolfi@ic.ac.uk)*
**** *Max-Planck-Institut für Dynamik komplexer technischer Systeme, Germany (e-mail: raisch@control.tu-berlin.de)*
◇ *Siemens AG, Germany (e-mail: tevfik.sezi@siemens.com)*

**Abstract:** We consider the problems of frequency stability, voltage stability and power sharing in droop–controlled inverter–based microgrids with meshed topologies and dominantly inductive power lines. Assuming that the conductances in the microgrid can be neglected, a port–Hamiltonian description of a droop–controlled microgrid is derived. The model is used to establish sufficient conditions for local stability. Furthermore, we propose a condition for the controller parameters such that a desired steady–state active power distribution is achieved. The robustness of the stability condition with respect to the presence of conductances is analyzed via a simulation example based on the CIGRE benchmark medium voltage distribution network.

*Keywords:* microgrid stability, inverters, droop control, port–Hamiltonian systems

## 1. INTRODUCTION

The increasing amount of renewable energy sources present in the electrical grid requires new technical concepts to ensure a safe and reliable operation. Two main reasons for this are: *(i)* most renewable generation sources are small–scale distributed generation (DG) units connected at the low (LV) and medium voltage (MV) levels; *(ii)* a large portion of these DG units are interfaced with the network via AC inverters, the physical characteristics of which largely differ from the characteristics of conventional synchronous generators (SGs).

In that regard, microgrids represent a promising near–time concept to facilitate the integration of renewable DG sources, see Lasseter (2002). A microgrid gathers a combination of generation units, loads and energy storage elements at distribution level into a locally controllable system, which can be operated in isolation from the main transmission system. A microgrid in the latter operation mode is called an autonomous or islanded microgrid.

This paper addresses three important performance criteria in such networks: frequency stability, voltage stability and power sharing. Here, power sharing is understood as the ability of the local controls of the individual generation sources to achieve a desired steady–state distribution of their power outputs *relative* to each other, while satisfying the load demand in the network. The relevance of this control objective lies within the fact that it allows to pre-specify the utilization of the generation units in operation.

⋆ Partial support from the HYCON2 Network of excellence (FP7 ICT 257462) is acknowledged.

A widely used, though heuristic, solution for the problem of active power sharing in conventional power systems is droop control, see Kundur (1994). In the case of an SG, droop control is a decentralized proportional control, which sets the mechanical output power in dependency of the relative deviations of the rotational speed of the SG. Given its successful application in such systems, this technique has been adapted to inverter–based networks in Chandorkar et al. (1993); Coelho et al. (2002).

Furthermore, the power lines in microgrids are typically relatively short. Then, slight differences in voltage amplitudes can lead to large reactive power flows and reactive power sharing among sources can not be ensured. Therefore, the automatic voltage regulator (AVR) used in conventional power systems to control the voltage amplitude at a generator bus to a nominal setpoint is, in general, not adequate in microgrids. This motivates the application of droop control to also achieve a desired reactive power distribution. In networks with dominantly inductive power lines, the most common approach is to control the voltage amplitude with a proportional control, the feedback signal of which is the reactive power generation relative to a reference setpoint, see Chandorkar et al. (1993); Coelho et al. (2002) and the recent survey Guerrero et al. (2013).

Stability analysis of droop–controlled microgrids has been traditionally carried out by means of detailed numerical small–signal analysis as well as extensive simulations and experimental studies aiming to characterize a range for the droop gains guaranteeing system stability, see Coelho et al. (2002); Pogaku et al. (2007).

Under the assumption of constant voltage amplitudes, conditions for frequency stability and power sharing for radial microgrids with first–order inverter models and purely inductive power lines have recently been presented in Simpson-Porco et al. (2013a). Conditions for voltage stability for a parallel microgrid with inductive power lines have been derived in Simpson-Porco et al. (2013b) under the assumption of small or constant angle differences.

However, and as pointed out in Guerrero et al. (2013), most work on microgrid stability has so far focussed on radial microgrids, while stability of microgrids with meshed topologies and decentralized controlled units is still an open research area. In that regard, and under the assumption of constant voltage amplitudes, analytic synchronization conditions for a lossy meshed microgrid with distributed rotational and electronic generation are derived in Schiffer et al. (2013) using ideas from second order consensus algorithms. A decentralized LMI–based control design for lossy meshed inverter–based networks guaranteeing overall network stability for a nonlinear model considering variable voltage amplitudes and phase angles is provided in Schiffer et al. (2012).

The main contribution of this paper is to give sufficient conditions on the control parameters to ensure local stability of droop–controlled inverter–based microgrids operated with the control laws given in Chandorkar et al. (1993). We hereby consider networks with general meshed topology and inverter models with variable frequencies as well as variable voltage amplitudes. Since the synchronization frequency is the same for all DG units and their dynamics depend on the angle differences, it is possible to translate—via a time–dependent coordinate shift—the synchronization objective into a (standard) equilibrium stabilization problem, which is the approach adopted here.

Specifically, we follow the interconnection and damping assignment passivity–based control approach of Ortega et al. (2002) to represent the lossless microgrid in port–Hamiltonian form, see van der Schaft (2000). This allows to easily identify the energy–Lyapunov function and give conditions for stability of the synchronization equilibrium state. In contrast to Simpson-Porco et al. (2013a,b); Schiffer et al. (2013), no assumptions of constant voltage amplitudes or small phase angle differences are made.

The remainder of the paper is organized as follows. The network model is presented in Section 2. The inverter model and the droop control are introduced in Section 3. Sufficient conditions for local stability for lossless microgrids are established in Section 4. In Section 5 we propose a selection of the droop gains and setpoints that ensures the DG units share (in steady–state) the active power according to a specified pattern. The robustness of our stability condition with respect to model uncertainties, *e.g.* conductances, is evaluated in Section 6 with a simulation example based on the CIGRE (Conseil International des Grands Réseaux Electriques) benchmark MV distribution network, see Rudion et al. (2006). The paper is wrapped–up with some conclusions and future work in Section 7.

This paper is an abridged version of Schiffer et al. (2014), in which further results on properties of droop–controlled microgrids, also under the presence of conductances, are given. These include, among others, a proof that for all practical choices of the parameters of the droop controllers global boundedness of trajectories is ensured. In addition, based on this result, a relaxed stability condition for a specific gain selection in a lossless network is derived. Furthermore, extensive simulation studies illustrating the theoretical analysis are provided.

**Notation.** We define the sets $\mathbb{R}_{\geq 0} := \{x \in \mathbb{R} | x \geq 0\}$, $\mathbb{R}_{>0} := \{x \in \mathbb{R} | x > 0\}$, $\mathbb{R}_{<0} := \{x \in \mathbb{R} | x < 0\}$, $\mathbb{S} := [0, 2\pi)$ and $\bar{n} := \{1, \dots, n\}$. Given a set $\mathcal{U} := \{\nu_1, \dots, \nu_n\}$, the notation $i \sim \mathcal{U}$ denotes "for all $i \in \mathcal{U}$". Let $x := \mathrm{col}(x_i) \in \mathbb{R}^n$ denote a vector with entries $x_i$ for $i \sim \bar{n}$, $\underline{0}_n \in \mathbb{R}^n$ the zero vector, $\mathbb{1}_n \in \mathbb{R}^n$ the vector with all ones and $\mathrm{diag}(a_i), i \sim \bar{n}$, an $n \times n$ diagonal matrix with diagonal entries $a_i$. Let $j$ denote the imaginary unit. The transpose of the gradient of a function $f : \mathbb{R}^n \to \mathbb{R}$ is denoted by $\nabla f$.

## 2. NETWORK MODEL

We consider a generic meshed network model in which loads are represented by constant impedances. This leads to a set of nonlinear differential–algebraic equations. It is then possible to eliminate all algebraic equations corresponding to loads via a process called Kron reduction, see Kundur (1994), and obtain a set of pure differential equations. We assume this process has been carried out and work with the Kron–reduced network.

In the Kron–reduced microgrid, composed of $n$ nodes, each node represents a DG unit interfaced via an AC inverter. We denote the set of network nodes by $\bar{n}$ and associate a time–dependent phase angle $\delta_i : \mathbb{R}_{\geq 0} \to \mathbb{S}$, as well as a time–dependent voltage amplitude $V_i : \mathbb{R}_{\geq 0} \to \mathbb{R}_{>0}$ to each node $i \in \bar{n}$ in the microgrid. We furthermore assume that the power lines of the microgrid are dominantly inductive. Then, two nodes $i$ and $k$ of the microgrid are connected via a complex nonzero admittance $Y_{ik} := G_{ik} + jB_{ik} \in \mathbb{C}$ with conductance $G_{ik} \in \mathbb{R}_{>0}$ and susceptance $B_{ik} \in \mathbb{R}_{<0}$. For convenience, we define $Y_{ik} := 0$ whenever $i$ and $k$ are not directly connected via an admittance. The set of neighbors of a node $i \in \bar{n}$ is given by $\mathcal{N}_i := \{k \mid k \in \bar{n},\ k \neq i\ , Y_{ik} \neq 0\}$. For ease of notation, we write angle differences as $\delta_{ik}(t) := \delta_i(t) - \delta_k(t)$ and define the vectors $\delta(t) := \mathrm{col}(\delta_i(t)) \in \mathbb{S}^n$, $\omega(t) := \mathrm{col}(\omega_i(t)) \in \mathbb{R}^n$ and $V(t) := \mathrm{col}(V_i(t)) \in \mathbb{R}^n$, where $\dot{\delta}(t) = \omega(t)$.

Following Kundur (1994), the overall active and reactive power flows $P_i : \mathbb{S}^n \times \mathbb{R}^n_{>0} \to \mathbb{R}$ and $Q_i : \mathbb{S}^n \times \mathbb{R}^n_{>0} \to \mathbb{R}$ at a node $i \in \bar{n}$ are given by[1]

$$\begin{aligned} P_i &= G_{ii}V_i^2 - \sum_{k \sim \mathcal{N}_i} V_i V_k (G_{ik}\cos(\delta_{ik}) + B_{ik}\sin(\delta_{ik})), \\ Q_i &= -B_{ii}V_i^2 - \sum_{k \sim \mathcal{N}_i} V_i V_k (G_{ik}\sin(\delta_{ik}) - B_{ik}\cos(\delta_{ik})), \end{aligned} \tag{1}$$

with

$$G_{ii} := \hat{G}_{ii} + \sum_{k \sim \mathcal{N}_i} G_{ik},\ B_{ii} := \hat{B}_{ii} + \sum_{k \sim \mathcal{N}_i} B_{ik}, \tag{2}$$

where $\hat{G}_{ii} \in \mathbb{R}_{>0}$ and $\hat{B}_{ii} \in \mathbb{R}_{<0}$ denote the shunt conductance, respectively shunt susceptance, at node $i$. The apparent power flow is given by $S_i = P_i + jQ_i$. We associate to each inverter its power rating $S_i^N \in \mathbb{R}_{>0}$, $i \sim \bar{n}$.

We assume that the microgrid is connected, *i.e.* that for all pairs $\{i, k\} \in \bar{n} \times \bar{n}$, $i \neq k$, there exists an ordered sequence of nodes from $i$ to $k$ such that any pair of consecutive nodes in the sequence are connected by a power line represented by an admittance. This assumption is reasonable for a microgrid, unless severe line outages separating the system into several disconnected parts occur. Since we are mainly concerned with dynamics of generation units, we express all power flows in "Generator Reference Arrow System".

[1] To simplify notation the time argument of all signals is omitted in the sequel.

## 3. INVERTER MODEL AND DROOP CONTROL

The inverters are modeled as AC voltage sources with controllable amplitude and frequency, see Lopes et al. (2006)[2]. The frequency regulation is assumed instantaneous, but the voltage control is assumed to happen with a delay represented by a first order filter with time constant $\tau_{V_i} \in \mathbb{R}_{>0}$. Then, the dynamics of the inverter at node $i \in \bar{n}$ can be modeled as

$$\begin{aligned} \dot{\delta}_i &= u_i^{\delta}, \\ \tau_{V_i} \dot{V}_i &= -V_i + u_i^{\mathrm{V}}, \end{aligned} \tag{3}$$

where $u_i^{\delta} : \mathbb{R}_{\geq 0} \to \mathbb{R}$ and $u_i^{V} : \mathbb{R}_{\geq 0} \to \mathbb{R}$ are controls. The active and reactive power outputs are assumed to be measured and passed through filters with time constant $\tau_{P_i} \in \mathbb{R}_{>0}$ and $P_i$ and $Q_i$ given in (1), see Coelho et al. (2002); Pogaku et al. (2007), *i.e.*

$$\begin{aligned} \tau_{P_i} \dot{P}_i^m &= -P_i^m + P_i, \\ \tau_{P_i} \dot{Q}_i^m &= -Q_i^m + Q_i. \end{aligned} \tag{4}$$

Differently from SGs, inverters do not have an inherent physical relation between frequency and generated active power. Droop control attempts at artificially establishing such relation, since it is desired in many applications, see Engler (2005). The typical (heuristic) argument for the derivation of the droop control laws for inverter–based systems with dominantly inductive power lines is as follows, see Chandorkar et al. (1993); Engler (2005). Assume dominantly inductive power lines, *i.e.* $G_{ik} \approx 0$, and small phase angle differences $\delta_{ik}$. Then, it follows from the power flow equations (1) that the active power flow $P_i$ is mainly affected by the phase angle differences, while the reactive power flow $Q_i$ is mostly influenced by differences in voltage amplitudes. This motivates proportional feedback laws coupling the frequency with the active power and the voltage with the reactive power, namely

$$\begin{aligned} u_i^{\delta} &= \omega^d - k_{P_i}(P_i^m - P_i^d), \\ u_i^{V} &= V_i^d - k_{Q_i}(Q_i^m - Q_i^d), \end{aligned} \tag{5}$$

where $\omega^d \in \mathbb{R}_{>0}$ is the desired (nominal) frequency, $V_i^d \in \mathbb{R}_{>0}$ the desired (nominal) voltage amplitude, $k_{P_i} \in \mathbb{R}_{>0}$ and $k_{Q_i} \in \mathbb{R}_{>0}$ are the frequency and voltage droop gains, $P_i^m : \mathbb{R}_{\geq 0} \to \mathbb{R}$ and $Q_i^m : \mathbb{R}_{\geq 0} \to \mathbb{R}$ the measured powers and $P_i^d \in \mathbb{R}$ and $Q_i^d \in \mathbb{R}$ their desired setpoints. Inserting (5) in (3) together with (4) yields the closed–loop system

$$\begin{aligned} \dot{\delta}_i &= \omega^d - k_{P_i}(P_i^m - P_i^d), \\ \tau_{P_i} \dot{P}_i^m &= -P_i^m + P_i, \\ \tau_{V_i} \dot{V}_i &= -V_i + V_i^d - k_{Q_i}(Q_i^m - Q_i^d), \\ \tau_{P_i} \dot{Q}_i^m &= -Q_i^m + Q_i. \end{aligned} \tag{6}$$

Since, in general, $\tau_{V_i} \ll \tau_{P_i}$, we assume $\tau_{V_i} = 0$ in the sequel. In addition, we rewrite the system (6) following Schiffer et al. (2013) and obtain

$$\begin{aligned} \dot{\delta}_i &= \omega_i, \\ \tau_{P_i} \dot{\omega}_i &= -\omega_i + \omega^d - k_{P_i}(P_i - P_i^d), \\ \tau_{P_i} \dot{V}_i &= -V_i + V_i^d - k_{Q_i}(Q_i - Q_i^d), \end{aligned} \tag{7}$$

[2] An underlying assumption to this model is that whenever the inverter connects an intermittent renewable generation source, *e.g.,* a photovoltaic plant or a wind plant, to the network, it is equipped with some sort of storage (*e.g.*, flywheel, battery). Thus, it can increase and decrease its power output in a certain range.

where $\omega_i$ denotes the inverter frequency. Defining

$$\begin{aligned} P^d &:= \mathrm{col}(P_i^d) \in \mathbb{R}^n,\ P := \mathrm{col}(P_i) \in \mathbb{R}^n, \\ Q^d &:= \mathrm{col}(Q_i^d) \in \mathbb{R}^n,\ Q := \mathrm{col}(Q_i) \in \mathbb{R}^n, \\ V^d &:= \mathrm{col}(V_i^d) \in \mathbb{R}^n,\ T := \mathrm{diag}(\tau_{P_i}) \in \mathbb{R}^{n \times n}, \\ K_P &:= \mathrm{diag}(k_{P_i}) \in \mathbb{R}^{n \times n},\ K_Q := \mathrm{diag}(k_{Q_i}) \in \mathbb{R}^{n \times n}, \end{aligned} \tag{8}$$

we can write the system (7) compactly as

$$\begin{aligned} \dot{\delta} &= \omega, \\ T\dot{\omega} &= -\omega + \mathbb{1}_n \omega^d - K_P(P - P^d), \\ T\dot{V} &= -V + V^d - K_Q(Q - Q^d), \end{aligned} \tag{9}$$

with power flows $P$ and $Q$ given in (1).

*Remark 3.1.* Note that $P_i^d$ can also take negative values whenever an inverter connects a storage device to the network. Then, the storage device functions as a frequency and voltage dependent load, which is charged in dependency of the excess power available in the network. We refer to such operation mode as charging mode.

*Remark 3.2.* There are several other alternative droop control schemes proposed in the literature, *e.g.,* Zhong (2013); Guerrero et al. (2013). The one given in (5) is the most common one for dominantly inductive networks. We therefore restrict our analysis to these control laws, commonly referred to as "conventional droop control".

## 4. STABILITY FOR LOSSLESS MICROGRIDS

In this section conditions for stability for *lossless microgrids*, *i.e.* $G_{ik} = 0$ for all $i \in \bar{n}$, $k \in \bar{n}$, are derived. We therefore make the following assumption on the network admittances.

*Assumption 4.1.* $G_{ik} = 0$ and $B_{ik} \leq 0$, $i \sim \bar{n}$, $k \sim \bar{n}$.

This assumption can be justified for certain microgrids, especially on the MV level, as follows: while the line admittance in MV and LV networks has usually a non–negligible resistive part, typically the inverter output impedance is inductive (due to the inductance of the output filter and/or the presence of an output transformer). Then, the inductive parts dominate the resistive parts.

We only consider such microgrids and absorb the inverter output admittance (together with the possible transformer admittance), $\tilde{Y}_{ik}$, into the line admittances, $Y_{ik}$, while neglecting all resistive effects. In the present case this assumption is further justified, since the droop control laws introduced in (5) are mostly used in networks with dominantly inductive admittances, see Guerrero et al. (2013).

Under Assumption 4.1, the power flows (1) reduce to

$$\begin{aligned} P_i &= \sum_{k \sim \mathcal{N}_i} |B_{ik}| V_i V_k \sin(\delta_{ik}), \\ Q_i &= |B_{ii}| V_i^2 - \sum_{k \sim \mathcal{N}_i} |B_{ik}| V_i V_k \cos(\delta_{ik}). \end{aligned}$$

*Remark 4.2.* The need to introduce the, sometimes unrealistic, assumption of lossless admittances has a long history in power systems studies. We are aware that in the case of the Kron–reduced network the reduced network admittance matrix does, in general, not permit to neglect the conductances and our stability results might therefore be inaccurate. An alternative is to consider the idealized scenario in which part of the inverter–interfaced storage devices operate in charging mode, hence acting as loads while all constant impedance loads are neglected. Another approach is to use other, possibly dynamic, load models

instead of constant impedances in the so–called structure preserving power system models. However, in the presence of variable voltages the load models are usually, somehow artificially, adapted to fit the theoretical framework used for the construction of energy–Lyapunov functions, see *e.g.,* Davy and Hiskens (1997).

To establish our main result we need the following natural assumption on existence of a synchronized motion of system (9).

*Assumption 4.3.* There exist constants $\delta^s \in \Theta$, $\omega^s \in \mathbb{R}$ and $V^s \in \mathbb{R}^n_{>0}$, where

$$\Theta := \left\{ \delta \in \mathbb{S}^n \mid |\delta_{ik}| < \frac{\pi}{2}, i \sim \bar{n},\ k \sim \mathcal{N}_i \right\},$$

such that the system (9) possesses for all $t \geq 0$ a synchronized motion given by[3]

$$\delta^*(t) = \mathrm{mod}_{2\pi}\{\delta^s + \underline{1}_n \omega^s t\},\ \omega^*(t) = \underline{1}_n \omega^s,\ V^*(t) = V^s, \quad (10)$$

satisfiying

$$\mathbb{1}_n \omega^s - \mathbb{1}_n \omega^d + K_P[P(\delta^s, V^s) - P^d] = 0,$$
$$V^s - V^d + K_Q[Q(\delta^s, V^s) - Q^d] = 0.$$

*Remark 4.4.* It is well–known that in lossless power systems $\sum_{i\sim\bar{n}} P_i^s = 0$. Hence, the synchronization frequency can be uniquely determined by replacing the synchronized motion (10) in (7) and adding up all nodes, yielding

$$\omega^s = \omega^d + \frac{\sum_{i\sim\bar{n}} P_i^d}{\sum_{i\sim\bar{n}} \frac{1}{k_{P_i}}}.$$

It follows that, for any $i \in \bar{n}$,

$$\omega^s - \omega^d - k_{P_i} P_i^d = \sum_{k\sim\bar{n}, k\neq i} \frac{k_{P_i}}{k_{P_k}} \left(\omega^d - \omega^s + k_{P_k} P_k^d\right). \quad (11)$$

### *4.1 Error dynamics*

To establish conditions on the setpoints and gains of the controller (5) such that the synchronized motion (10) is stable, it is convenient to introduce the error coordinates

$$\tilde{\omega}(t) := \omega(t) - \mathbb{1}_n \omega^s, \quad \tilde{\delta}(t) := \delta(0) + \int_0^t \tilde{\omega}(\tau) d\tau$$

and to study stability of the synchronized motion (10) in the coordinates $\mathrm{col}(\tilde{\delta}(t), \tilde{\omega}(t), V(t)) \in \mathbb{R}^n \times \mathbb{R}^n \times \mathbb{R}^n_{>0}$.

Note that the power flows $P$ and $Q$ in (8) are invariant to a uniform shift of all angles. Hence, $\delta^*$ is only unique up to such a shift and convergence to the desired synchronized motion (10) (up to a uniform shift of all angles) does not depend on the value of the angles, but only on their differences. Therefore, we can arbitrarily choose one node, say the $n$–th node, as a reference node, express $\tilde{\delta}_i$, $i \in \bar{n} \setminus \{n\}$ relative to $\tilde{\delta}_n$ via the state transformation

$$\theta := \mathcal{R}\tilde{\delta}, \quad \mathcal{R} := [I_{(n-1)} \ -\mathbb{1}_{(n-1)}] \quad (12)$$

and study convergence to the synchronized motion (10) in the reduced system of order $3n-1$ with $\theta = \mathrm{col}(\theta_1, \ldots, \theta_{n-1})$ replacing $\tilde{\delta}$.

To simplify notation, we define the *constant*[4] $\theta_n := 0$, the shorthand $\theta_{ik} := \theta_i - \theta_k$ (which clearly verifies $\theta_{ik} \equiv \delta_{ik}$ for $k \neq n$ and $\theta_{in} \equiv \theta_i$) and the constants

$$c_{1_i} := \omega^d - \omega^s + k_{P_i} P_i^d,\ c_{2_i} := V_i^d + k_{Q_i} Q_i^d,\ i \sim \bar{n}. \quad (13)$$

[3] The operator $\mathrm{mod}_{2\pi}\{\cdot\} : \mathbb{R} \to [0, 2\pi)$, is defined as follows: $y = \mathrm{mod}_{2\pi}\{x\}$ yields $y = x - k2\pi$ for some integer $k$ with $\mathrm{sign}(y) = \mathrm{sign}(x)$ and $y \in [0, 2\pi)$.

[4] The constant $\theta_n$ is not part of the state vector $\theta$.

In the new coordinates $\mathrm{col}(\theta, \tilde{\omega}, V) \in \mathbb{R}^{n-1} \times \mathbb{R}^n \times \mathbb{R}^n_{>0}$ the dynamics (9) take for the $i$–th node, $i \in \bar{n} \setminus \{n\}$, the form

$$\dot{\theta}_i = \tilde{\omega}_i - \tilde{\omega}_n,$$
$$\tau_{P_i} \dot{\tilde{\omega}}_i = -\tilde{\omega}_i - k_{P_i} \sum_{k\sim\mathcal{N}_i} V_i V_k |B_{ik}| \sin(\theta_{ik}) + c_{1_i}, \quad (14)$$
$$\tau_{P_i} \dot{V}_i = -V_i - k_{Q_i} \big(|B_{ii}| V_i^2 - \sum_{k\sim\mathcal{N}_i} V_i V_k |B_{ik}| \cos(\theta_{ik})\big) + c_{2_i},$$

while the dynamics of the reference node $n$ are given by

$$\tau_{P_n} \dot{\tilde{\omega}}_n = -\tilde{\omega}_n + k_{P_n} \sum_{k\sim\mathcal{N}_n} V_n V_k |B_{nk}| \sin(\theta_k) + c_{1_n}, \quad (15)$$
$$\tau_{P_n} \dot{V}_n = -V_n - k_{Q_n} \big(|B_{nn}| V_n^2 - \sum_{k\sim\mathcal{N}_n} V_n V_k |B_{nk}| \cos(\theta_k)\big) + c_{2_n}.$$

This reduced system has an equilibrium at

$$x^s := \mathrm{col}(\theta^s, \underline{0}_n, V^s), \quad (16)$$

the asymptotic stability of which implies asymptotic convergence of all trajectories of the system (9) to the synchronized motion (10) up to a uniform shift of all angles.

### *4.2 Main result*

To present the main stability result it is convenient to introduce the matrices $\mathcal{L} \in \mathbb{R}^{(n-1)\times(n-1)}$, $\mathcal{W} \in \mathbb{R}^{(n-1)\times n}$, $\mathcal{D} \in \mathbb{R}^{n\times n}$ and $\mathcal{T}(\theta^s) \in \mathbb{R}^{n\times n}$ defined in Appendix A.

*Lemma 4.5.* Consider system (9), (1) with Assumptions 4.1 and 4.3. Then $\mathcal{L} > 0$.

**Proof.** Consider the vector $P$ defined in (8) under Assumption 4.1 and let $\tilde{L}$ be given by

$$\tilde{L} := \frac{\partial P}{\partial \delta}\Big|_{(\delta^s, V^s)} \in \mathbb{R}^{n\times n}$$

with entries given in Appendix A. Under the given assumptions, and recalling that the microgrid is connected by assumption, $\tilde{L}$ is a symmetric Laplacian matrix of a connected graph with the properties, see Simpson-Porco et al. (2013a); Schiffer et al. (2013)

$$\tilde{L}\gamma\mathbb{1}_n = 0,\ v^\top \tilde{L} v > 0,\ \forall v \in \mathbb{R}^n \setminus \{v = \gamma\mathbb{1}_n\},\ \gamma \in \mathbb{R}. \quad (17)$$

Recall the matrix $\mathcal{R}$ defined in (12), let $r := \begin{bmatrix}\underline{0}^\top_{(n-1)} & 1\end{bmatrix}$ and note that

$$\tilde{L} \begin{bmatrix}\mathcal{R} \\ r\end{bmatrix}^{-1} = \tilde{L} \begin{bmatrix} I_{(n-1)} & \mathbb{1}_{(n-1)} \\ \underline{0}^\top_{(n-1)} & 1 \end{bmatrix} = \begin{bmatrix} \mathcal{L} & \underline{0}_{n-1} \\ b^\top & 0 \end{bmatrix}, \quad (18)$$

where $b = \mathrm{col}(\tilde{l}_{in}) \in \mathbb{R}^{(n-1)}$, $i \sim \bar{n} \setminus \{n\}$. It follows from (17) and (18) that for any $\tilde{v} := \mathrm{col}(\vartheta, 0) \in \mathbb{R}^n$, $\vartheta \in \mathbb{R}^{(n-1)}$

$$\tilde{v}^\top \tilde{L} \begin{bmatrix}\mathcal{R} \\ r\end{bmatrix}^{-1} \tilde{v} = \tilde{v}^\top \tilde{L} \tilde{v} = \vartheta^\top \mathcal{L} \vartheta > 0.$$

Moreover, $\mathcal{L}$ is symmetric. Hence, $\mathcal{L} > 0$.

We are now ready to state our main result.

*Proposition 4.6.* Consider the system (9), (1) with Assumptions 4.1 and 4.3. Fix $\tau_{P_i}$, $k_{P_i}$ and $P_i^d$. Select $V_i^d, k_{Q_i}$ and $Q_i^d$ such that

$$\mathcal{D} + \mathcal{T}(\theta^s) - \mathcal{W}^\top \mathcal{L}^{-1} \mathcal{W} > 0. \quad (19)$$

Then the equilibrium $x^s = \mathrm{col}(\theta^s, \underline{0}_n, V^s)$ of system (14)–(15) is locally asymptotically stable.

**Proof.** Following the interconnection and damping assignment passivity–based control approach of Ortega et al. (2002), we establish the claim by representing the system (14)–(15) in port–Hamiltonian form to identify the

energy–Lyapunov function. Defining $x := \mathrm{col}(\theta, \tilde{\omega}, V)$, the system (14)–(15) can be written as

$$\dot{x} = (J - R(x))\nabla H \tag{20}$$

with Hamiltonian $H : \mathbb{R}^{(n-1)} \times \mathbb{R}^n \times \mathbb{R}^n_{>0} \to \mathbb{R}$ given by

$$H(x) = \sum_{i=1}^{n} \Big( \frac{\tau_{P_i}}{2k_{P_i}} \tilde{\omega}_i^2 + \frac{1}{k_{Q_i}}(V_i - c_{2_i} \ln(V_i)) + \frac{1}{2}|B_{ii}|V_i^2 - \frac{1}{2} \sum_{k \sim \mathcal{N}_i} V_i V_k |B_{ik}| \cos(\theta_{ik}) \Big) - \sum_{i=1}^{n-1} \frac{c_{1_i}}{k_{P_i}} \theta_i. \tag{21}$$

The interconnection and damping matrices are

$$J = \begin{bmatrix} 0_{(n-1)\times(n-1)} & \mathcal{J} \\ -\mathcal{J}^\top & 0_{2n\times 2n} \end{bmatrix}, \; R = \mathrm{diag}(\underline{0}_{(n-1)}, R_\omega, R_V),$$

where $\mathcal{J} = \begin{bmatrix} \mathcal{J}_K & -\frac{k_{P_n}}{\tau_{P_n}} \mathbb{1}_{(n-1)} & 0_{(n-1)\times n} \end{bmatrix}$,

$$\mathcal{J}_K = \mathrm{diag}\left( \frac{k_{P_k}}{\tau_{P_k}} \right) \in \mathbb{R}^{(n-1)\times(n-1)}, \; k \sim \bar{n} \setminus \{n\},$$

$$R_\omega = \mathrm{col}\left( \frac{k_{P_i}}{\tau_{P_i}^2} \right) \in \mathbb{R}^n, \; R_V = \mathrm{col}\left( \frac{k_{Q_i} V_i}{\tau_{P_i}} \right) \in \mathbb{R}^n,$$

$i \sim \bar{n}$. Notice that $J = -J^\top$ and $R \geq 0$ and hence

$$\dot{H} = -(\nabla H)^\top R \nabla H \leq 0. \tag{22}$$

Consequently, $x^s$ is a stable equilibrium of system (14)–(15) if $H(x)$ has a strict local minimum at the equilibrium $x^s$. The latter can be ensured by showing that $\nabla H(x^s) = \underline{0}_{(3n-1)}$ and $\frac{\partial^2 H(x)}{\partial x^2}\big|_{x^s} > 0$. That the first requirement is satisfied follows from

$$\left( \frac{\partial H}{\partial \theta}\Big|_{x^s} \right)^\top = \mathrm{col}\big(a_i - \frac{c_{1_i}}{k_{P_i}}\big) \in \mathbb{R}^{(n-1)}, \quad \left( \frac{\partial H}{\partial \tilde{\omega}}\Big|_{x^s} \right)^\top = \underline{0}_n,$$

$$\left( \frac{\partial H}{\partial V}\Big|_{x^s} \right)^\top = \mathrm{col}\left( -b_l + |B_{ll}|V_l^s + \frac{1}{k_{Q_l}} \left( 1 - \frac{c_{2_l}}{V_l^s} \right) \right) \in \mathbb{R}^n,$$

where $i \sim \bar{n} \setminus \{n\}$, $l \sim \bar{n}$ and

$$a_i := \sum_{k \sim \mathcal{N}_i} V_i^s V_k^s |B_{ik}| \sin(\theta_{ik}^s), \; b_l := \sum_{k \sim \mathcal{N}_l} V_k^s |B_{lk}| \cos(\theta_{lk}^s).$$

Evaluating the Hessian of $H(x)$ at $x^s$ yields

$$\frac{\partial^2 H(x)}{\partial x^2}\Big|_{x^s} = \begin{bmatrix} \mathcal{L} & 0_{(n-1)\times n} & \mathcal{W} \\ 0_{n\times(n-1)} & \mathcal{A} & 0_{n\times n} \\ \mathcal{W}^\top & 0_{n\times n} & \mathcal{D} + \mathcal{T}(\theta^s) \end{bmatrix}$$

where $\mathcal{L}$, $\mathcal{W}$, $\mathcal{D}$ and $\mathcal{T}(\theta^s)$ are given in (A.1), (A.2) and $\mathcal{A} := \mathrm{diag}(\tau_{P_i}/k_{P_i}) \in \mathbb{R}^{n\times n}$. Since $\mathcal{A}$ is positive definite, the Hessian is positive definite if and only if the submatrix

$$\begin{bmatrix} \mathcal{L} & \mathcal{W} \\ \mathcal{W}^\top & \mathcal{D} + \mathcal{T}(\theta^s) \end{bmatrix} \tag{23}$$

is positive definite. Now, Lemma 4.5 implies that, under the standing assumptions, $\mathcal{L}$ is positive definite. Hence, the matrix (23) is positive definite if and only if

$$\mathcal{D} + \mathcal{T}(\theta^s) - \mathcal{W}^\top \mathcal{L}^{-1} \mathcal{W} > 0,$$

which is condition (19). Note that from (2), it follows that $\mathcal{T}(\theta^s)$ is positive semidefinite.

From (22) and the fact that $R(x) \geq 0$, it follows that the equilibrium $x^s$ is asymptotically stable if

$$R(x(t))\nabla H(x(t)) \equiv \underline{0}_{(3n-1)} \; \Rightarrow \lim_{t\to\infty} x(t) = x^s \tag{24}$$

along the trajectories of the system (20). This implies

$$\frac{\partial H}{\partial \tilde{\omega}} = \underline{0}_n, \; \frac{\partial H}{\partial V} = \underline{0}_n.$$

The first condition implies $\tilde{\omega} = \underline{0}_n$ and, hence, $\theta$ is constant. The second condition implies $V$ constant. Consequently, the invariant set where $\dot{H}(x(t)) \equiv 0$ is an equilibrium. To prove that this is the desired equilibrium $x^s$ we recall that $x^s$ is an isolated minimum of $H(x)$. Hence, there is a neighborhood of $x^s$ where no other equilibrium exists, completing the proof.

Condition (19) has the following physical interpretation: the droop control laws (5) establish a feedback interconnection linking the phase angles $\delta$, respectively $\theta$, with the active power flows $P$, as well as the voltages $V$ with the reactive power flows $Q$.

The matrices $\mathcal{L}$ and $\mathcal{T}(\theta^s)$ represent then the network coupling strengths between the phase angles and the active power flows, respectively, the voltages and the reactive power flows. In the same way, $\mathcal{W}$ can be interpreted as a local cross–coupling strength originating from the fact that $P \neq P(\delta)$ and $Q \neq Q(V)$, but $P = P(\delta, V)$ and $Q = Q(\delta, V)$.

Condition (19) states that to ensure local stability of the equilibrium $x^s$ defined in (16) the couplings represented by $\mathcal{L}$ and $\mathcal{T}(\theta^s)$ have to dominate over the cross–couplings of the power flows contained in $\mathcal{W}$. If that is not the case the voltage variations have to be reduced by reducing the magnitudes of the gains $k_{Q_i}$, $i \in \bar{n}$.

Another possibility is to adapt $Q_i^d$ and $V_i^d$. This does, however, not seem as appropriate in practice since these two parameters are typically setpoints provided by a supervisory control, which depend on the nominal voltage of the network and the expected loading conditions.

*Remark 4.7.* To see that (20) is indeed an equivalent representation of (14)–(15), note that the part of the dynamics of $\tilde{\omega}_n$ in (15) resulting from $J\nabla H$ is

$$\frac{k_{P_n}}{\tau_{P_n}} \mathbb{1}_{(n-1)}^\top \left( \frac{\partial H}{\partial \theta} \right)^\top = \frac{k_{P_n}}{\tau_{P_n}} \Big( \sum_{k \sim \mathcal{N}_n} V_n V_k |B_{nk}| \sin(\theta_k) - \sum_{i=1}^{n-1} \frac{c_{1_i}}{k_{P_i}} \Big),$$

since $\sum_{i=1}^{n-1} \sum_{k \sim \mathcal{N}_i, k \neq n} V_i V_k |B_{ik}| \sin(\theta_{ik}) = 0$. From (11), we moreover have that

$$c_{1_n} = \omega^d - \omega^s + k_{P_n} P_n^d = -\sum_{i=1}^{n-1} \frac{k_{P_n}}{k_{P_i}} c_{1_i}.$$

The remaining term in $\tilde{\omega}_n$ is contributed by the dissipation part $R\nabla H$.

*Remark 4.8.* The analysis reveals that stability properties of the lossless microgrid (9) are independent of the frequency droop gains $k_{P_i}$, the active power setpoints $P_i^d$ and the low pass filter time constants $\tau_{P_i}$, and only condition (19) is imposed on $V_i^d, k_{Q_i}$ and $Q_i^d$. In that regard, the result is identical to those derived for lossless first–order inverter models in Simpson-Porco et al. (2013a) and lossless second–order inverter models in Schiffer et al. (2013), both assuming constant voltage amplitudes.

## 5. ACTIVE POWER SHARING

Following the ideas derived in Simpson-Porco et al. (2013a), we derive a selection criterion for the controller gains and setpoints such that the generation units share the active power according to a user–defined performance criterion in steady–state. We employ the following definition to formulate the selection criterion.

*Definition 5.1.* Let $\chi_i \in \mathbb{R}_{>0}$ denote weighting factors and $P_i^s$ the steady–state active power flow, $i \sim \bar{n}$. Then, two inverters at nodes $i$ and $k$ are said to share their active powers proportionally if

$$\frac{P_i^s}{\chi_i} = \frac{P_k^s}{\chi_k}. \tag{25}$$

A possible power sharing performance criterion would be, for example, $\chi_i = S_i^N$, $i \sim \bar{n}$, where $S_i^N \in \mathbb{R}_{>0}$ is the nominal power rating of inverter $i$.

*Lemma 5.2.* Consider the system (9), (1). Assume that it possesses a synchronized motion with synchronization frequency $\omega^s \in \mathbb{R}_{>0}$. Then all inverters, the power outputs of which satisfy $\text{sign}(P_i^s) = \text{sign}(P_k^s)$, achieve proportional active power sharing if the gains $k_{P_i}$ and $k_{P_k}$ and the active power setpoints $P_i^d$ and $P_k^d$ are chosen such that

$$k_{P_i}\chi_i = k_{P_k}\chi_k \text{ and } k_{P_i}P_i^d = k_{P_k}P_k^d, \tag{26}$$

$i \sim \bar{n}$ and $k \sim \bar{n}$.

**Proof.** The claim follows in a straighforward manner from Simpson-Porco et al. (2013a), where it has been shown for first–order inverter models and $\chi_i = S_i^N$, $P_i^d > 0$, $P_i^s > 0$, $i \sim \bar{n}$. Under conditions (26), we have along the synchronized motion of the system (9)

$$\frac{P_i^s}{\chi_i} = \frac{-\omega^s + \omega^d + k_{P_i}P_i^d}{k_{P_i}\chi_i} = \frac{-\omega^s + \omega^d + k_{P_k}P_k^d}{k_{P_k}\chi_k} = \frac{P_k^s}{\chi_k},$$

where $i \in \bar{n}$ and $k \in \bar{n}$ with $\text{sign}(P_i^s) = \text{sign}(P_k^s)$.

Lemma 5.2 guarantees proportional active power sharing independently of the admittance values of the network. Moreover, Lemma 5.2 also ensures that storage devices in charging mode are charged proportionally.

*Remark 5.3.* As described in Section 3, the voltage droop control law (5) follows a similar heuristic approach as the frequency control droop law, aiming at obtaining a desired reactive power distribution in steady–state. However, the voltage droop control (5) does in general not achieve proportional reactive power sharing since – unlike the frequency – in general $V_i^s \neq V_k^s$ for $i \in \bar{n}$ and $k \in \bar{n}$.

## 6. SIMULATION EXAMPLE

We illustrate the theoretical analysis via a simulation example based on the three–phase islanded Subnetwork 1 of the CIGRE benchmark medium voltage distribution network, see Rudion et al. (2006). The network represents a meshed microgrid composed of 11 main buses, see Fig. 1. It possesses six controllable generation sources of which two are batteries at buses 5b ($i = 1$) and 10b ($i = 5$), two are FCs in households at buses 5c ($i = 2$) and 10c ($i = 6$) and two are FC CHPs at buses 9b ($i = 3$) and 9c ($i = 4$). We assume that all controllable generation units are equipped with frequency and voltage droop control as given in (5) and associate to each inverter its power rating $S_i^N = [0.505, 0.028, 0.261, 0.179, 0.168, 0.012]$ pu, where pu denotes per unit values with respect to the system base power $S_{\text{base}} = 4.75$ MVA. The maximum system load is $0.91 + j0.30$ pu. The total PV generation is 0.15 pu. A detailed model description together with further simulation studies are given in Schiffer et al. (2014).

The simulation also serves to evaluate the robustness of the model (1), (9) and the stability condition (19) with respect to model uncertainties. In that regard, the inductances are modeled by first–order ODEs opposed to constant admittances as in (1). Furthermore, loads are represented by impedances. The simulation is carried out in Plecs.

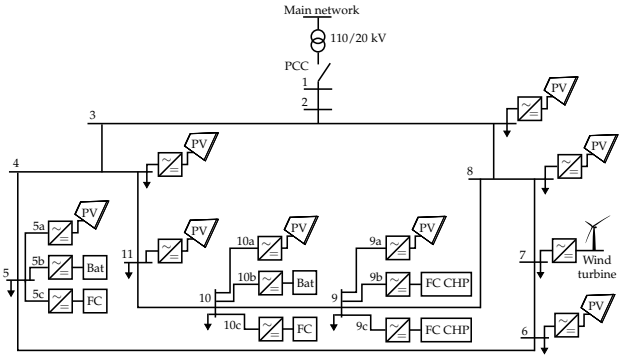


Fig. 1. Benchmark model adapted from Rudion et al. (2006) with 11 main buses and inverter–interfaced units of type: PV–Photovoltaic, FC–fuel cell, Bat–battery, FC CHP. PCC denotes the point of common coupling to the main grid. The sign ↓ denotes loads.

We treat PV generation as negative loads and assume all PV units work at 50% of their nominal power. The wind turbine is neglected. To determine the equivalent admittance of a load at a node $i \in \bar{n}$, the load demand and PV generation at each bus are added and the admittance value is calculated at nominal frequency and voltage ($V_{\text{base}} = 20$ kV). In the corresponding Kron–reduced network all nodes represent controllable DGs.

The largest $R/X$ ratio of an element of the admittance matrix of the equivalent Kron–reduced network is 0.22, while a typical value for an HV transmission line is 0.31, see Engler (2005). Consequently, the assumption of dominantly inductive admittances is satisfied and the droop control laws (5) are appropriate. The active power droop gains and setpoints of the inverters are designed according to Lemma 5.2 with $\chi_i = S_i^N$, $P_i^d = \alpha_i S_i^N$ pu, $k_{P_i} = 0.1/S_i^N$ Hz/pu and $\alpha_i = 0.65$, $i \sim \bar{n}$. The reactive power setpoints are set to $Q_i^d = \beta_i S_i^N$ pu with $\beta_i = 0.25$, $i \sim \bar{n}$ and the reactive power droop gains are chosen in the same relation as the active power droop gains, *i.e.* $k_{Q_i} = 0.2/S_i^N$ pu/pu and $V_i^d = 1$ pu, $i \sim \bar{n}$. The low pass filter time constants are set to $\tau_{P_i} = 0.5$ s, $i \sim \bar{n}$.

The simulation results in Fig. 2 show that all trajectories synchronize in less than 3 s. Condition (19) is satisfied, which indicates that the condition is robust – to a certain extent – to the presence of transfer and load conductances. As predicted by Lemma 5.2, the active power is shared proportionally by the droop–controlled sources. The voltage amplitudes satisfy the typical requirement of $0.9 < V_i^s < 1.1$ for $V_i^s$ in pu and $i \sim \bar{n}$. However, the reactive power sharing among all units is not proportional.

The observation that the stability condition (19) is, to a certain extent, robust to the presence of model uncertainties is reconfirmed in numerous further simulation scenarios with a large variety of different parameter settings.

## 7. CONCLUSIONS

We have considered the problems of frequency stability, voltage stability and power sharing in a droop–controlled inverter–based microgrid with dominantly inductive power lines. Based on a port–Hamiltonian representation of the microgrid (derived under the assumption of negligible conductances) we have established a sufficient condition for local stability, which depends on the choice of the controller

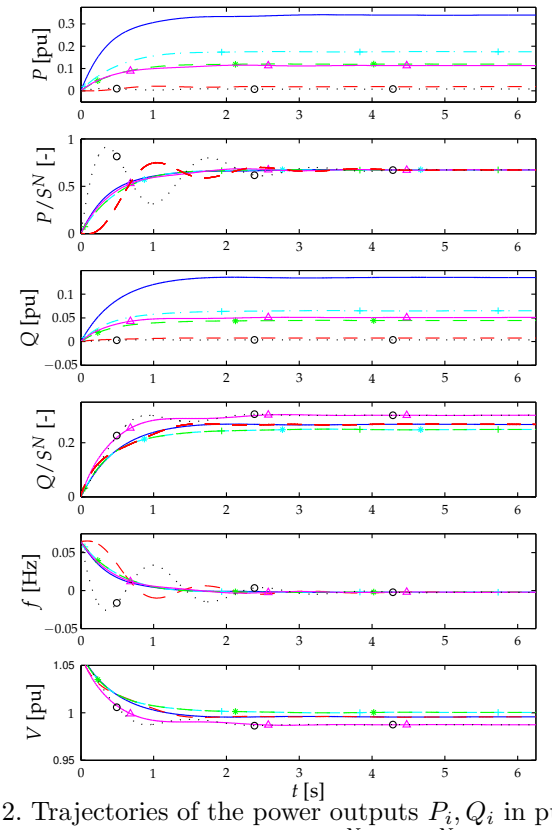


Fig. 2. Trajectories of the power outputs $P_i, Q_i$ in pu, the relative power outputs $P_i/S_i^N, Q_i/S_i^N$, the internal relative frequencies $f_i = (\omega_i - \omega^d)/(2\pi)$ in Hz and the voltage amplitudes $V_i$ in RMS of the controllable sources in the microgrid given in Fig. 1. The lines correspond to: battery 5b, $i = 1$ '–', FC 5c, $i = 2$ '- -', FC CHP 9b, $i = 3$ '+-', FC CHP 9c, $i = 4$ '* -', battery 10b, $i = 5$ '△ -' and FC 10c, $i = 6$ 'o-'.

gains and setpoints of the voltage droop controllers, but does neither depend on the choices of the controller gains and setpoints of the frequency droop controllers nor on the low pass filter time constants. A design criterion on the controller gains and setpoints guaranteeing a desired steady–state active power distribution has been provided.

The robustness of the stability condition with respect to model uncertainties, such as the presence of conductances, has been evaluated in a simulation example based on the CIGRE benchmark MV distribution network. The simulations show that the derived stability condition is satisfied and a desired steady–state active power distribution is achieved for a wide selection of different control gains, setpoints, low pass filter time constants and initial conditions.

Since droop control fails in general to achieve a desired reactive power distribution, future research concerns alternative, possibly distributed, solutions to this problem.

## Appendix A. DEFINITION OF THE MATRICES $\mathcal{D}$, $\tilde{L}$, $\mathcal{L}$, $\mathcal{W}$ AND $\mathcal{T}(\theta^S)$

The matrix $\mathcal{D}$ is given by

$$\mathcal{D} := \operatorname{diag}\left(\frac{c_{2_m}}{k_{Q_m}(V_m^s)^2}\right) = \operatorname{diag}\left(\frac{V_m^d + k_{Q_m}Q_m^d}{k_{Q_m}(V_m^s)^2}\right), m \sim \bar{n}. \tag{A.1}$$

The entries of the matrices $\tilde{L}, \mathcal{L}, \mathcal{W}$ and $\mathcal{T}(\theta^s)$ are given by

$$\tilde{l}_{pp} := \sum_{q=1}^{n} |B_{pq}|V_p^s V_q^s \cos(\delta_{pq}^s), \tilde{l}_{pq} := -|B_{pq}|V_p^s V_q^s \cos(\delta_{pq}^s),$$
$$l_{ii} := \sum_{q=1}^{n} |B_{iq}|V_i^s V_q^s \cos(\theta_{iq}^s),\ l_{ik} := -|B_{ik}|V_i^s V_k^s \cos(\theta_{ik}^s),$$
$$w_{ii} := \sum_{q=1}^{n} |B_{iq}|V_q^s \sin(\theta_{iq}^s),\ w_{iq} := |B_{iq}|V_i^s \sin(\theta_{iq}^s),$$
$$t_{pp} := |B_{pp}|, \quad t_{pq} := -|B_{pq}|\cos(\theta_{pq}^s), \tag{A.2}$$

where $i \sim \bar{n} \setminus \{n\}$, $k \sim \bar{n} \setminus \{n\}$, as well as $p \sim \bar{n}$ and $q \sim \bar{n}$.

## REFERENCES

Chandorkar, M., Divan, D., and Adapa, R. (1993). Control of parallel connected inverters in standalone AC supply systems. *IEEE Trans. on Ind. Appl.*, 29(1), 136 –143.

Coelho, E., Cortizo, P., and Garcia, P. (2002). Small-signal stability for parallel-connected inverters in standalone AC supply systems. *IEEE Trans. on Industry Applications*, 38(2), 533 –542.

Davy, R.J. and Hiskens, I.A. (1997). Lyapunov functions for multimachine power systems with dynamic loads. *IEEE Trans. on Circuits and Systems I*, 44(9), 796–812.

Engler, A. (2005). Applicability of droops in low voltage grids. *Int. Journal of Distr. Energy Resources*, 1(1), 1–6.

Guerrero, J., Loh, P., Chandorkar, M., and Lee, T. (2013). Advanced control architectures for intelligent microgrids – part I: Decentralized and hierarchical control. *IEEE Trans. on Industrial Electronics*, 60(4), 1254–1262.

Kundur, P. (1994). *Power system stability and control*. McGraw-Hill.

Lasseter, R. (2002). Microgrids. In *IEEE Power Engineering Society Winter Meeting*, volume 1, 305 – 308.

Lopes, J., Moreira, C., and Madureira, A. (2006). Defining control strategies for microgrids islanded operation. *IEEE Trans. on Power Systems*, 21(2), 916 – 924.

Ortega, R., van der Schaft, A., Maschke, B., and Escobar, G. (2002). Interconnection and damping assignment passivity-based control of port-controlled Hamiltonian systems. *Automatica*, 38(4), 585–596.

Pogaku, N., Prodanovic, M., and Green, T. (2007). Modeling, analysis and testing of autonomous operation of an inverter-based microgrid. *IEEE Trans. on Power Electronics*, 22(2), 613 –625.

Rudion, K., Orths, A., Styczynski, Z., and Strunz, K. (2006). Design of benchmark of medium voltage distribution network for investigation of DG integration. In *IEEE PESGM*, 6 pp.

Schiffer, J., Anta, A., Trung, T.D., Raisch, J., and Sezi, T. (2012). On power sharing and stability in autonomous inverter-based microgrids. In *Proc. 51st IEEE CDC*. Maui, HI, USA.

Schiffer, J., Goldin, D., Raisch, J., and Sezi, T. (2013). Synchronization of droop-controlled microgrids with distributed rotational and electronic generation. In *Proc. 52nd IEEE CDC*. Florence, Italy.

Schiffer, J., Ortega, R., Astolfi, A., Raisch, J., and Sezi, T. (2014). Conditions for stability of droop–controlled inverter–based microgrids. *Automatica*. Accepted.

Simpson-Porco, J.W., Dörfler, F., and Bullo, F. (2013a). Synchronization and power sharing for droop-controlled inverters in islanded microgrids. *Automatica*, 49(9), 2603 – 2611.

Simpson-Porco, J.W., Dörfler, F., and Bullo, F. (2013b). Voltage stabilization in microgrids using quadratic droop control. In *Proc. 52nd IEEE CDC*. Florence, Italy.

van der Schaft, A. (2000). *L2-Gain and Passivity Techniques in Nonlinear Control*. Springer.

Zhong, Q.C. (2013). Robust droop controller for accurate proportional load sharing among inverters operated in parallel. *IEEE Trans. on Ind. Electr.*, 60(4), 1281–1290.